Aerobic oxidation of 5-hydroxymethylfurfural into 2,5-furandicarboxylic acid in water under mild conditions

Journal:	*Green Chemistry*
Manuscript ID:	GC-ART-10-2014-002019.R1
Article Type:	Paper
Date Submitted by the Author:	13-Nov-2014

Complete List of Authors:	Liu, Bing; South-Central University for Nationalities, key Laboratory of Catalysis and Material Sciences of the State Ethnic Affairs Commission & Ministry of Education Ren, Yongshen; South-Central University for Nationalities, key Laboratory of Catalysis and Material Sciences of the State Ethnic Affairs Commission & Ministry of Education Zhang, Zehui; South-Central University for Nationalities, key Laboratory of Catalysis and Material Sciences of the State Ethnic Affairs Commission & Ministry of Education

Pd/C@Fe_3O_4 catalyst showed high catalytic activity in the oxidation of 5-hydroxymethylfurfural into 2,5-furandicarboxylic acid under mild reaction conditions

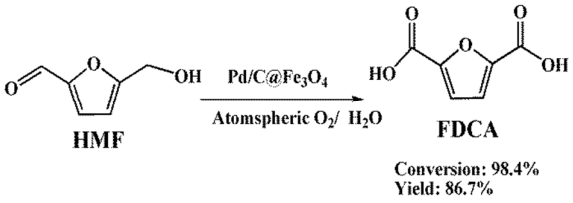

Cite this: DOI: 10.1039/c0xx00000x

www.rsc.org/xxxxxx

ARTICLE TYPE

Aerobic oxidation of 5-hydroxymethylfurfural into 2,5-furandicarboxylic acid in water under mild conditions

Bing Liu*, Yongshen Ren, and Zehui Zhang*

Received (in XXX, XXX) Xth XXXXXXXXX 20XX, Accepted Xth XXXXXXXXX 20XX

DOI: 10.1039/b000000x

In this study, Pd nanoparticles were immobilized on the core-shell structure C@Fe_3O_4 (carbon is shell, and Fe_3O_4 is the core) magnetic microspheres via in situ adsorption and reduction to generate magnetically separable Pd/C@Fe_3O_4 catalyst. In this method, no excess reductant and capping reagents were required, which is a clean, simple and green process for the preparation of magnetic Pd nanocatalyst. The Pd/C@Fe_3O_4 catalyst showed high activity and extraordinary stability for the oxidation of biomass derived 5-hydroxymethylfurfural (HMF) into 2,5-furandicarboxylic acid (FDCA) under mild conditions. A study for optimizing the reaction conditions such as reaction temperature, reaction solvent and base amount has been performed. Under optimal reaction conditions, HMF conversion of 98.4% and FDCA yield of 86.7% were achieved after 6 h at 80 ^oC. After reaction, the Pd/C@Fe_3O_4 catalyst could be easily recovered by an external magnet and reused without the loss of its activity.

Introduction

Nowadays, there has been a growing interest in search of renewable resources to replace non-renewable fossil resources for the production of energy and chemicals. Biomass is the only carbon-containing renewable resource, and it is abundant in quantity as a substitute for fossil fuels.[1-2] Currently, much effort has been devoted to the conversion of biomass into useful chemicals and valuable fuels.[3-5] 5-Hydroxymethylfurfural (HMF) can be readily generated from the dehydration of various carbohydrates such as fructose, glucose, and cellulose.[6-9] HMF can be used as a promising precursor for the synthesis of bulk chemicals, fine chemicals, polymers and liquid fuels. Therefore, HMF has been identified as one of the key platform chemicals to bridge biomass and fossil resources.[10, 11] Oxidation of HMF can generate several important furan chemicals such as 2,5-diformylfuran (DFF), 5-hydroxymethyl-2-furancarboxylic acid (HMFCA) and 2,5-furandicarboxylic acid (FDCA).[12-14] The structure of FDCA is similar with that of terephthalic acid, which is obtained from fossil resources and used as a monomer in the synthesis of polymers. Thus FDCA can be used as a potential biorenewable monomer to replace terephthalic acid in the production of polyethylene terephthalate (PET).[15] In addition, FDCA has also been used as value added intermediate for the production of biomass-derived chemicals.[16]

In early reports, synthesis of FDCA was obtained by the oxidation of HMF using stoichiometric oxidants such as $KMnO_4$.[17] However, the cost was high and large amount of waste was released to the environment. Later, the oxidation of HMF into FDCA was catalyzed by homogeneous metal salts (Co^{2+}/Mn^{2+}/Br^-) under high pressure (70 bar air).[18] However, the use of the homogeneous catalysts showed some drawbacks such as the difficulty in catalyst recycle and the toxic pollution to environment. Therefore, great effort has been devoted to design heterogeneous catalysts for the oxidation of HMF into FDCA. A number of previous publications reported the oxidation of HMF to FDCA principally was mainly catalyzed by Pt, Pd, and Au-based catalysts.[19-21] For example, Rass et al. demonstrated that HMF was quantitatively oxidized to FDCA over C/Pt catalyst at 100 ℃ under 40 bar air with Na_2CO_3/HMF molar ratio = 2.[21] Davis et al. reported full HMF conversion were achieved by the use of Pd/C and Pt/C catalysts with FDCA yields between 71% and 79% under 690 kPa O_2 pressure.[22] Compared with other metal nanoparticles, supported Au catalysts showed encouraging catalytic performance and were received much more attention. For example, Corma et al. reported that oxidation of HMF over Au/CeO_2 catalyst afforded nearly quantitative FDCA yield at 130 ^oC under 1 MPa air pressure and high concentration of NaOH (Mole ratio of NaOH/HMF = 4).[23] However, Au/CeO_2 catalyst

Department of Chemistry, Key Laboratory of Catalysis and Material Sciences of Ministry of Education. South-Central University for Nationalities MinYuan Road 182, Wuhan, R.P. China E-mail: liubing@mail.scuec.edu.cn; zhangzehui@mail.scuec.edu.cn

was not stable, and its catalytic activity decreased rapidly in the second run. Davis et al. reported that full HMF conversion and FDCA yield of 65% were obtained by the use of high NaOH/HMF mole ratio of 20 over Au/TiO_2 under 345 kPa oxygen.[24] Most of the previous reported methods required hash reaction conditions such as high pressure, high temperature or high base concentration. Acknowledging these important achievements, it is still a challenge to develop new catalytic methods for the oxidation of HMF to FDCA under comparatively mild reaction conditions.

The growing demand for environment-friendly chemical processes has impelled many researchers to develop heterogeneous catalysts, which can be facilely recovered and reused. Recently, magnetically recyclable catalysts have proved to be a kind of promising ones combining the advantages of high activity and facile recovery.[25] Among various magnetic materials, core-shell structure $C@Fe_3O_4$ composites have particularly been attracted great interest.[26, 27] In comparison to the common silica shells, carbon shells exhibit superior properties such as much higher stability in acid or base media, as well as at high temperatures and pressures.[28] More importantly, large amounts of functional groups such as hydroxyl group and carboxylic groups can be easily generated on the surface of carbon, which could make a contribution to the adsorption of heavy metal ions and stabilize metal nanoparticles.[29] For example, Makowski et al. reported that hydrophilic carbon spheres supported Pd nanoparticles showed high catalytic activity in the hydrogenation of phenol to cyclohexanone.[30]

Considering the obvious difficulty in the recycle of the small size carbon particles, herein, the core-shell structure $C@Fe_3O_4$ microspheres were prepared by hydrothermal method, and used to immobilize of Pd nanocatalysts ($Pd/C@Fe_3O_4$). The as-prepared $Pd/C@Fe_3O_4$ catalyst was used for the aerobic oxidation of HMF into FDCA in water under mild reaction conditions.

Experimental Section

Materials

$FeCl_3.6H_2O$ (99.5 %), polyvinylpyrrolidone (99.0%), ethylene glycol (99.0 %), sodium acetate (99.0 %) and glucose (99.5%) were purchased from Sinopharm Chemical Reagent Co., Ltd. (Shanghai, China). Acetonitrile (HPLC grade) was purchased from Tedia Co. (Fairfield, USA). Sodium tetrachloropalladate(II) (98.0%) (Na_2PdCl_4) was purchased from Aladdin Chemicals Co. Ltd. (Beijing, China). HMF (98%) was purchased from Beijing Chemicals Co. Ltd. (Beijing, China). DFF and FDCA were purchased from the J&K Chemical Co. Ltd., (Beijing, China). All the solvents were purchased from Sinopharm Chemical Reagent Co., Ltd. (Shanghai, China). All the chemicals were of analytical grade and used without further purification. Ultrapure water was used for the catalyst preparation and catalytic reactions.

Preparation of core-shell structure $C@Fe_3O_4$ composites

Core-shell structure $C@Fe_3O_4$ composites were prepared according to the known method with a slight modification.[31] Solvothermal of $FeCl_3.6H_2O$ in ethylene glycol in the presence of polyvinylpyrrolidone and sodium acetate at 200 ^oC for 8 h generated black Fe_3O_4 microspheres. The as-prepared Fe_3O_4 microspheres were homogeneously dispersed in an aqueous solution of glucose with an assist of sonication, and then the mixture was heated at 200 ^oC for 12 h to produce $C@Fe_3O_4$ microspheres.

Preparation of $Pd/C@Fe_3O_4$ catalyst

$C@Fe_3O_4$ microspheres (80 mg) were homogeneously dispersed in ethylene glycol (50 mL) with an assist of for 30 minutes. Then Na_2PdCl_4 (12 mg) in ethylene glycol (5 mL) was added dropwise. The mixture was further heated at 105 ^oC for another 3 h under a vigorous stirring. After cooling to room temperature, the catalyst was collected by an external magnet and washed several times with deionized water to remove the physically absorbed ions. Finally, the purified catalyst was dried in a vacuum oven overnight. The palladium deposited $C@Fe_3O_4$ microspheres were abbreviated as $Pd/C@Fe_3O_4$ in the following.

Catalyst Characterization

Nitrogen adsorption isotherms were measured with an Autosorb-1 (Quantachrome, USA) at 77 K. Prior to the measurement, all the sample was degassed at 200 ^oC for 6 h in a vacuum line. The BET surface area was determined by a multipoint BET method using the adsorption data in the relative pressure (P/P_0) range of 0.05–0.3. The mesoporous pore size distributions were derived from desorption branches of isotherms by using BJH model. Transmission electron microscope (TEM) images were obtained using an FEI Tecnai G^2-20 instrument. The sample powder were firstly dispersed in ethanol and dropped onto copper grids for observation. X-ray powder diffraction (XRD) patterns of samples were determined with a Bruker advanced D8 powder diffractometer (Cu Kα). All XRD patterns were collected in the 2θ range of 10–80° with a scanning rate of 0.016°/s. X-ray photoelectron spectroscopy (XPS) was conducted on a Thermo VG scientific ESCA MultiLab-2000 spectrometer with a monochromatized Al Kα source (1486.6 eV) at constant analyzer pass energy of 25 eV. The binding energy was estimated to be accurate within 0.2 eV. All binding energies (BEs) were corrected referencing to the C1s (284.6 eV) peak of the contamination carbon as an internal standard. FT-IR measurements were recorded on a Nicolet NEXUS-6700 FTIR spectrometer with a spectral resolution of 4 cm^{-1} in the wave number range of 500-4000 cm^{-1}. The Pd content in the Fe_3O_4@C-Pd catalyst was quantitatively determined by inductively coupled atomic emission spectrometer (ICP-AES) on an IRIS Intrepid II XSP instrument (Thermo Electron Corporation).

General procedure for the oxidation of HMF over Fe_3O_4@C-Pd catalyst

Typically, HMF (50.4 mg, 0.4 mmol) and K_2CO_3 (0.5 equiv, 27.6 mg) were firstly dissolved in water (8 mL). Then Fe_3O_4@C-Pd (40 mg) was added and dispersed in the above solution by sonication. After that, oxygen was flowed at a rate of 20 mL min^{-1} from the bottom of the reactor, and the reaction mixture was stirred at 80 ^oC at a constant rate of 600 revolutions per minute (rpm) for a certain time. Time zero was recorded when the oxygen was flowed into the reaction mixture. The reaction was

monitored and analyzed by characterizing the reaction mixture using HPLC method.

Analytic methods

Products analysis was performed on a ProStar 210 HPLC system. Furan compounds were separated by a reversed-phase C18 column (200 × 4.6 mm) and detected by a UV detector at a wavelength of 280 nm. Acetonitrile and 0.1 wt.% acetic acid aqueous solution with the volume ratio of 30:70 was used as the mobile phase, and the flow rate was 1.0 mL min^{-1}. The content of furan compounds in samples was obtained directly by interpolation from calibration curves.

HMF conversion and FDCA yield are defined as follows:

HMF conversion = moles of HMF/moles of starting HMF ×100%

FDCA yield = moles of FDCA/moles of starting HMF ×100%

Recycling of catalyst

After reaction, the Pd/C@Fe_3O_4 catalyst was collected by a permanent magnet and washed several times with deionized water and ethanol three times, respectively. The spent catalyst was then dried under vacuum at 50 ^oC overnight, and then it was reused for the next cycle under the same reaction conditions.

Results and Discussion

Catalyst preparation and characterization

Scheme 1 illustrates the procedure of the synthesis of the magnetic Pd/C@Fe_3O_4 catalyst. Fe_3O_4 microspheres were prepared by the solvothermal method using $FeCl_3$ as precursor in ethylene glycol. The core-shell structure C@Fe_3O_4 microspheres were prepared by the in situ carbonization of glucose on the surface of Fe_3O_4 microspheres. Under hydrothermal conditions, the surface of the carbon layer was enriched with multiple functional groups such as hydroxyl and carboxylic acid groups. Thus, C@Fe_3O_4 microspheres can be used to anchor Pd^{2+} by the interaction between the oxygen-containing groups with Pd^{2+} to form ligand-substituted complex.[32, 33] The immobilized Pd^{2+} was solvothermally reduced to Pd nanoparticles by ethylene glycol,[34] and stabilized by oxygen-containing groups on the surface of C@Fe_3O_4 microspheres. The Pd content was determined to be 3.85 wt.% by ICP-AEC. It is worth noting that the Pd/C@Fe_3O_4 catalyst can be well dispersed in water, which facilitates the substrate to contact the active sites of the catalyst adequately for chemical reactions in water. The texture of the prepared catalyst was carried by the N_2 adsorption-desorption isotherms. The BET surface area and pore size were determined to be 18 m^2 g^{-1}, and 0.6 m^3 g^{-1}, respectively.

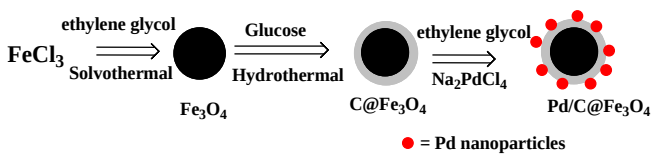

Scheme 1 Schematic illustration for the synthesis of Pd/C@Fe_3O_4 catalyst.

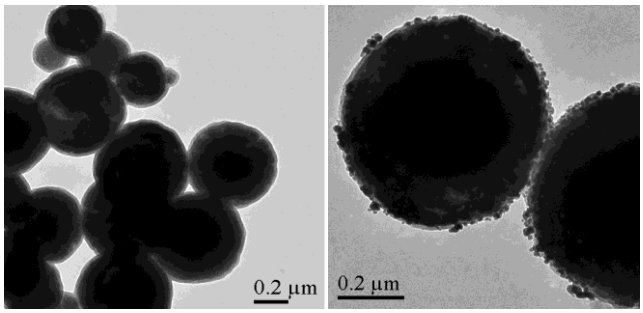

Figure. 1 TEM images of the C@Fe_3O_4 microspheres (a) and the Pd/C@Fe_3O_4 catalyst (b).

The morphology of C@Fe_3O_4 and Pd/C@Fe_3O_4 was characterized by TEM technology. Figure 1 (a) presents the typical TEM images of the as-synthesized C@Fe_3O_4 composite. The obtained C@Fe_3O_4 microspheres exhibited a relatively uniform size of 600 nm. However, some C@Fe_3O_4 microspheres with small diameter were also observed. As shown in Figure 3 (a), core-shell structure C@Fe_3O_4 microspheres were clearly observed after the hydrothermal of glucose in the presence of Fe_3O_4 microparticles. The dark Fe_3O_4 microspheres were coated with a grey layer of carbon with the shell thickness of about 20 nm. TEM image of a typical Pd/C@Fe_3O_4 microsphere is presented in Figure 1 (b). Due to the presence of numerous functional groups such as carbonyl and hydroxyl moieties on the surface of C@Fe_3O_4 microspheres, Pd nanoparticles were successfully anchored on the carbon shell of the C@Fe_3O_4 microspheres. As shown in Figure 1 (b), Pd nanoparticles were not uniform in size. Some aggregation of Pd nanoparticles were also observed. As far as the Pd nanoparticles size, it can be estimated from the full width at half maximum of a peak in the diffraction pattern of the nanoparticle according to Scherrer's equation (as shown in the following), and the average crystallite size of Pd nanoparticles size was determined to be 10 nm.

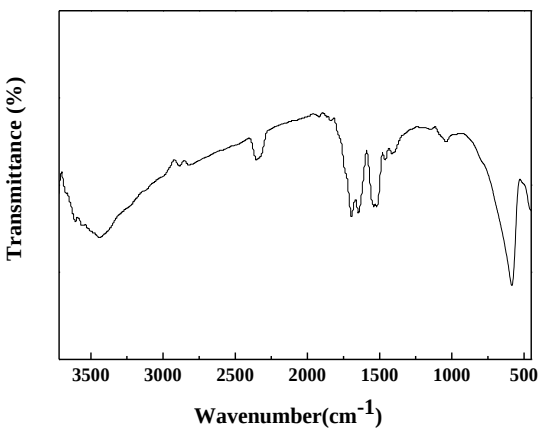

Figure **2.** FTIR spectra of the Pd/C@Fe_3O_4 catalyst.

In order to provide more information about the surface functional groups of the prepared Pd/C@Fe_3O_4 catalyst, it was further characterized by FT-IR technology. As shown Figure 2, a strong absorption peak at 586 cm^{-1} was the characteristic absorption band of Fe–O,[35] suggesting Fe_3O_4 was present in the catalyst. The band observed at 1640 cm^{-1} was assigned to the stretching vibration of C=C. [36] In addition, these peaks of 1400, 1450 and 1500 cm^{-1} were the characteristic vibration aromatic ring, which supported an aromatization of glucose during the hydrothermal treatment.[36] The absorption peak at 1700 was assigned to the stretching vibration of C=O and it was verified the presence of carboxylic group (-COOH).[36] The band at 3400 cm^{-1} was attributed to the stretching vibration of O–H band. The band at 1040 cm-1 was assigned to the C-OH stretching vibration. Through the FI-IR analysis, after the hydrothermal reaction, there were large numbers of hydrophilic functional groups (mainly including –COOH, and –C-OH) on the surface of C@Fe_3O_4, which facilitated the absorption of Pd^{2+} on the C@Fe_3O_4 surface and then immobilized Pd nanopartiles. The surface atomic ratio of oxygen and Pd in the catalyst was determined to be 15.8 by XPS. This result clearly indicated that the surface oxygen group was enough to anchor the Pd nanoparticles.

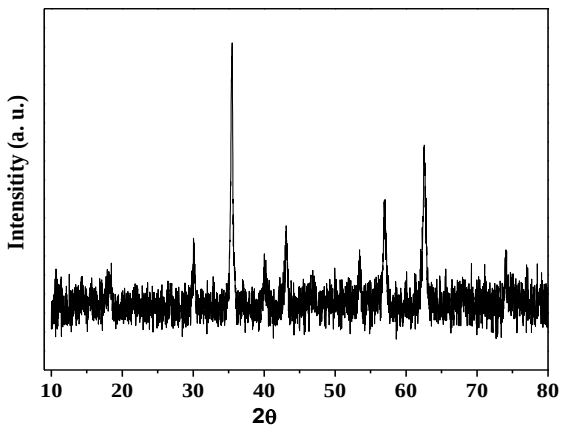

Figure 3. XRD diffraction patterns of the Pd/C@Fe_3O_4 microspheres.

XRD pattern of the Pd/C@Fe_3O_4 catalyst is shown in Figure 3. Diffraction peaks at 2θ = 30.1°, 35.5°, 43.1°, 53.6, 57.0°, and 63.3 ° were assigned to (220), (311), (400), (422), (511) and (440) Bragg reflections of face-centered cubic lattice of Fe_3O_4, which matched well with the standards of Fe_3O_4 (JCPDS 65-3107).[37] For the Pd nanoparticles, three peaks at 2θ = 40°, 47° and 68° were the characteristic diffraction peaks of the face centered cubic crystalline phase of palladium nanoparticles. The intensity of the peak at 2θ = 40° was much stronger than the other two peaks.[38] As shown in Figure 3, a peak at 2θ = 40.1° was observed, which was attributed to the interplanar-spacing for the 111 of Pd (0). The disappearance of the peaks at 2θ = 47° and 68° was mainly due to the lower weight percentage as compared with Fe_3O_4.

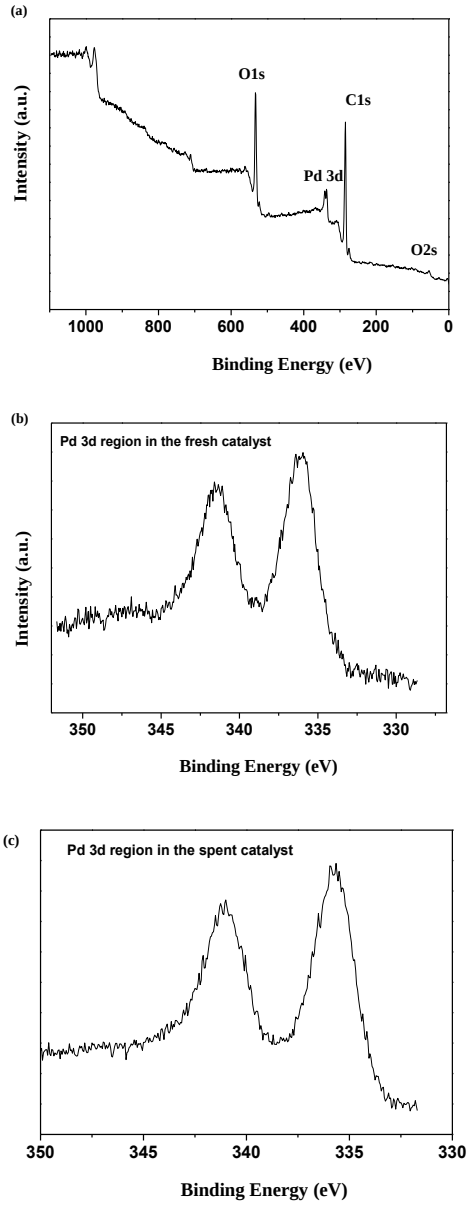

Figure 4. XPS spectra of the Fe_3O_4@C-Pd microspheres. (a) Survey scan of Pd/C@Fe_3O_4; (b) Pd 3d region in the fresh catalyst; (c) Pd 3d region in the spent catalyst;

XPS is a powerful tool to study the external surface of catalysts. XPS study is able to determine the chemical composition and oxidation degrees of components present on the catalyst surface. Therefore XPS technology was employed to investigate the surface chemical composition and valence state of the element Pd. Figure 4(a) shows the survey scan spectrum of the Pd/C@Fe_3O_4 catalyst. These peaks with a binding energy of about 285, 531, and 338 eV were attributed to C 1s, O 1s, and Pd 3d, respectively, which confirmed elements C, O and Pd were present on the surface of the catalyst. Meanwhile abundant C and O species indicated the presence of versatile oxygen-containing functional groups on the surface after the hydrothermal reaction of glucose. The confirmation of Fe_3O_4 by XPS technology was usually by the

observation of the characteristic Fe $2p_3/2$ and Fe $2p_{1/2}$ of Fe^{2+}, which had a high binding energy at 711.9 and 725.3 eV, respectively.[39] As shown in Figure 4, the two peaks were not observed in the XPS survey spectrum, suggesting that Fe_3O_4 was successfully coated with a carbon shell. High resolution XPS spectrum of Pd 3d is shown in Figure 4(b). Two peaks with binding energies of 335.8 and 341.2 eV were observed in Figure 4(b), which were assigned to Pd $3d_{5/2}$ and Pd $3d_{3/2}$, respectively. The two peaks were the characteristic peaks of metallic Pd, similar to that seen in Pd/C or Pd powder.[40]

The valence state of the Pd nanoparticle in the spent catalyst was also analyzed by XPS technology. As shown in Figure 4(c), there was no difference in the Pd 3d between the fresh catalyst and the spent catalyst. After reaction, Pd was still present in the form of metallic state. That is the reason our prepared catalyst showed a high stability during the catalyst recycling experiments. Our results were consistent with those previous results, in which they also found the supported Pd nanoparticles were stable for the oxidation of alcohols.[41] Although Pd nanopartilces are exposed to oxygen during the oxidation reactions, they have the risk to be oxidized to high valence state Pd^{2+}. Even though some part of Pd(0) was oxidized into Pd^{2+}, the Pd^{2+} could be reduced by solvent or substrate (alcohol) to Pd(0). For example, Zhang et al., recently reported that the organic ligands stabilized Pd^{2+} showed high catalytic activity for the oxidation of alcohol with molecular oxygen and they found that some Pd^{2+} was reduced to metallic Pd(0) after reaction.[42]

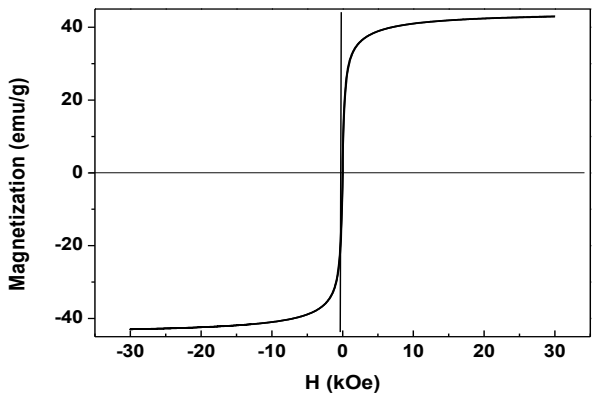

Figure 5. Hysteresis loops for the Pd/C@Fe_3O_4 catalyst at 300 K

Magnetic measurement of the Pd/C@Fe_3O_4 catalyst was carried out by a vibrating sample magnetometer (VSM) and the isothermal magnetization curve of the Pd/C@Fe_3O_4 catalyst is shown in Figure 5. The measurement was conducted at 300 K in the applied magnetic field from −30000 to +30000 Oe. As illustrated in Figure 5, the isothermal magnetization curve showed a rapid increase with the increase of the applied magnetic field. The saturated magnetization value of the catalyst was determined to be 42.7 emu g^{-1}. The superparamagnetic property of Fe_3O_4@C-Pd catalyst not only benefited their dispersibility and redispersibility in the solution, but also guaranteed the quick response of these nanoparticles to external magnetic fields, which should be promising in the in practical applications.

Catalytic aerobic oxidation of HMF in various solvents

Table 1. The results of HMF aerobic oxidation in different solvents

Entry	Solvent	HMF conversion (%)	FDCA yield (%)	DFF yield (%)
1	Toluene	5.9	0	4.7
2	Acetonitrile	9.7	0	8.6
3	Dimethyl sulfoxide	15.5	0	4.2
4	Ethanol	19.1	16.1	1.2
5	H_2O	86.5	76.9	3.2
6[b]	H_2O	20.6	11.9	7.1

[a] Reaction conditions: HMF (50.4 mg, 0.4 mmol), H_2O (8 mL), Pd/C@Fe_3O_4 (40 mg), K_2CO_3 (27.6 mg, 0.2 mmol), oxygen flow rate (30 mL min^{-1}), 80 °C, 4 h.
[b] The reaction was carried out in the absence of K_2CO_3.

To evaluate the catalytic activity of the as-prepraed Pd/C@Fe_3O_4 catalyst, aerobic oxidation of HMF was used as a model reaction. It is konwn that various solvents have different properties such as polarity, dielectric constant, steric hindrance, acid-base property, which would affect chemical reactions.[43] Therefore, experiments were initially carried out in various solvents to screen the best reaction medium. In addition, 0.5 equiv of K_2CO_3 was also used as additive, as the oxidation of alcohol over Pd based catalysts generally required the use of base. As shown in Table 1, HMF conversion was low in toluene and acetonitrile. (Table 1, Entries 1-2). One of the main reasons was that K_2CO_3 was insoluble in toluene and acetonitrile, which blocked the catalytic acitivity of Pd/C@Fe_3O_4. DFF was obtained in a relatively high selectivity without the formation of FDCA, indicating other side reactions such as the degradation of HMF was not obvious. Although HMF conversion was slightly improved to 15.5% in dimethyl sulfoxid (Table 1, Entry 3), DFF was the only product with a low selectivity of 27.1%. Interestingly, It is noted that FDCA was the major product when reactions were carried out in the protonic solvents (Table 1, Entris 4 & 5). However, the catalytic activity of Pd/C@Fe_3O_4 in ethanol and H_2O was quite different. Low HMF conversion of 19.1% and FDCA yield of 16.1% were obtained in ethanol (Table 1, Entry 4), while the reaction in water produced high HMF conversion of 86.5% and FDCA yield of 76.9% (Table 1, Entry 5). It is quite appealing to use H_2O as the solvent for the synthesis of important chemicals from biomass based chemicals, due to its low cost and without toxic pollution in line with green chemistry. In addition, control experiment was also carried out in water without K_2CO_3. Compared with the results in the presence of K_2CO_3, HMF conversion and FDCA selectivity greatly decreased without K_2CO_3 (Table 1, Entries 5 *vs* 6). These results clearly indicated that the base played a crucial

role in the aerobic oxidation of HMF into FDCA over $Pd/C@Fe_3O_4$ catalyst.

One important reason is for the use of base in the oxidation of HMF to FDCA is that base was used to neutralize the dicarboxylic acid (FDCA), as FDCA can be absorbed on the surface of metal nanoparticles. The salt of FDCA was dissolved in the reaction solution, and kept the catalyst activity stable. In fact, most of the reported methods required to use excessive NaOH (2~20 mole times of HMF). For example Davis et al. reported that full HMF conversion and FDCA yield of 65% were obtained by the use of high NaOH/HMF mole ratio of 20.[24] In our developed method, we just only required the stoichiometric amount of K_2CO_3 to netrulize FDCA in theroy, which greatly decreased the release of the waste to the envrioment.

Effect of base amount on the aerboic oxidation of HMF

In order to give more insights into the role of K_2CO_3 on the oxidation of HMF into FDCA over $Pd/C@Fe_3O_4$ catalyst, expriments were carried out in water at 80 °C with different amounts of the catalyst. As shown in Figure 6, HMF conversion and FDCA yield simultaneously increased with the incrase of the base loading. HMF conversion greatly improved from 34.9% with K_2CO_3/HMF mole ratio of 0.125 to 63.1% with with K_2CO_3/HMF mole ratio of 0.25. Further incrasing K_2CO_3/HMF mole ratio to 0.5, HMF conversion further increased to 86.5%. The change trend of FDCA yield was similar with that of HMF conversion. Besides the major product FDCA, DFF was also detected as one of the oxidation product. It is intresting to note that the ratio of FDCA and DFF (also FDCA selectivity) gradually increased with the increase of base amount. 0.5 equiv of K_2CO_3 (K_2CO_3/HMF mole ratio = 0.5) is the stoichiometric amount to neutralize the resultant FDCA in theroy. These results clearly indicated that K_2CO_3 indeed promoted the oxidation of HMF into FDCA in water over $Pd/C@Fe_3O_4$ catalyst. As reported by others on the role of base in the oxidation of HMF over supported Au nanocatalyst,[23,24] the base was used to timely neutralize the produced FDCA. Thus the use of base can avoid FDCA to adsorb on the surface of the Pd nanoparticles, keeping the catalytic activity of $Pd/C@Fe_3O_4$ catalyst stable.

When the mole ratio of K_2CO_3/HMF was further ehanced to 1, full HMF conversion was obtained. However, FDCA yield in this case was close to that with 0.5 equiv of K_2CO_3. It should be noted that the K_2CO_3 have a dual effect on this reaction. As it known to us, HMF was is stable under acidic or alkaline conditions due to the co-presence of the aldehyde and hydroxyl group in its structure. For instance, Rass et al. also found that the treatment of Na_2CO_3 (2 equiv) aqueous solution of HMF at 100 °C resulted in HMF degradation upto 50% after 2 h.[44] Therefore, too much use of K_2CO_3 also accelerated the degradation of HMF besides the promotion of the oxidation reaction, and K_2CO_3/HMF mole ratio of 0.5 was appropriate amount (the stoichiometric amount to neutralize the FDCA).

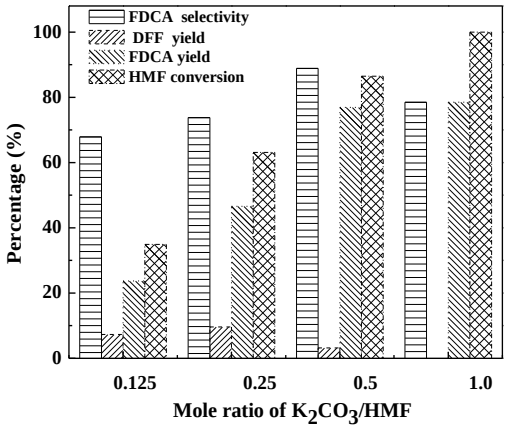

Figure 6. The results of HMF oxidation with different amount of K_2CO_3. Reaction conditions: HMF (50.4 mg, 0.4 mmol), H_2O (8 mL), $Pd/C@Fe_3O_4$ (40 mg), oxygen flow rate (30 mL min^{-1}), 80 °C, 4 h.

Effect of reaction temperature on the oxidation of HMF

With the aim to optimize the reaction conditions to get the highest FDCA yield, oxidation of HMF was also carried out at different reaction temperatures in the range from 298 K to 373 K, and the results are show in Table 2. It is worth noting that the aerobic oxidation of HMF was sensitive to the reaction temperature. The higher the reaction temperature was, the higher the HMF conversion was. Low HMF conversion of 28.6% was obtained at 25 °C. HMF conversion greatly enhanced from 28.6% to 60.1% by the increase of the reaction temperature from 25 to 50 °C. Further inceasing the reaction temperature to 80 °C, HMF conversion still greatly increased to 86.5%. Full HMF conversion was achieved at a 100 °C. Much more molecules would contact with catalyst active sites at higher reaction temperature. Therefore, HMF conversion increased with an increase of reaction temperature. Besides HMF conversion, FDCA selectivity was also greatly affected by the reaction temperaure. FDCA and DFF were both formed during the oxidation of HMF. It was found that the ratio of FDCA to DFF (FDCA selectivty) increased with the increase of reaction temperature from 298 K to 353 K (Table 2, Entries 1~3). Thsese results indicated that high reaction temperature not only promoted the oxidation of HMF into DFF, but also benefited the following oxidation of DFF into FDCA. However, the selectivity of FDCA at 100 °C was a little lower than that obtained at 80 °C (Table 3, Entries 3 *vs* 5). The highest FDCA yield was obtained in 86.7% after 6 h at the reaction temperature of 80 °C (Table 3, Entry 4). Although HMF conversion at 100 °C was a little high than that at 80 °C, FDCA yield at 100 °C was a little lower than taht at 80 °C. The possible reason should be that the degradation of HMF was much more serious at higher reaction temperature of 100 °C. As we mentioned above, HMF molecule contain s three functional groups such as hydroxyl group, aldehyde group, and furan ring, it was not stable in acidic or alkaline solution, which can degraded into humins. Vuyyuru et al. [45] found HMF was degraded into

humins (dark brwon color) and the degradation became more serious with the increase of the reaction temperature.

Table 2 The results of HMF oxidation at different reaction temperatures

Entry	Reaction temperature (^{o}C)	HMF conversion (%)	FDCA yield (%)	DFF yield (%)	FDCA selectivity (%)
1	25	28.6	11.9	15.1	41.6
2	50	60.1	36.6	18.9	60.9
3	80	86.5	76.9	3.2	88.9
4[b]	80	98.4	86.7	1.3	88.1
5	100	100	83.6	0	83.6

[a] Reaction conditions: HMF (50.4 mg, 0.4 mmol), H_2O (8 mL), K_2CO_3 (27.6 mg, 0.2 mmol). Pd/C@Fe_3O_4 (40 mg), oxygen flow rate (30 mL min^{-1}), 4 h.
[b] The reaction temperature was 6 h under otherwise the same reaction conditions as above.

Catalyst recycling experiments

The recycle and stability are two important characteristics for the use of heterogeneous catalysts. Therefore, the recycling experiments of the Pd/C@Fe_3O_4 catalyst were studied. The oxidation of HMF at 80 ^{o}C with the use of 0.5 equiv of K_2CO_3 was used as the model reaction. After reaction, the Fe_3O_4@C-Pd catalyst could be easily collected by an external magnet, washed successively with water and ethanol, followed by drying in vacuum at 50 ℃. The magnetic recycle of the catalyst can avoid the weight loss of the catalyst, which usually occurs in filtration processes. As shown in Figure 7, FDCA yields were almost stable after five consecutive cycles. However, there was still a very little decrease of FDCA yield. FDCA yield in the first run was 86.7%, and that was 83.7% in the fifth run. In addition, HMF conversion was also observed to show a very little decrease from 98.4% in the first run and 94.6% in the fifth run. We have determined the content of Pd in the spent catalyst after the fifth run, and calculated that the total weight percentage of Pd was lost about 2.3% after the fifth run.

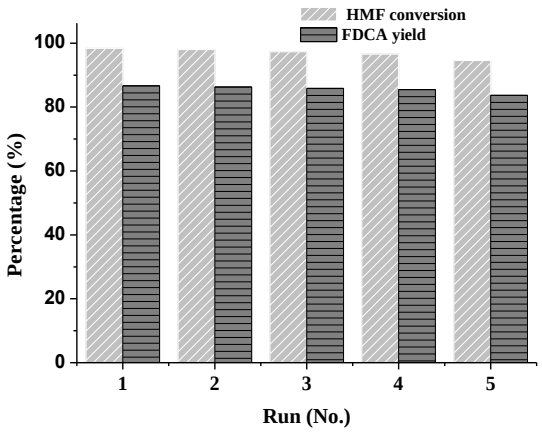

Figure 7 Recycle experiments of the Fe_3O_4@C-Pd catalyst. Reaction conditions: HMF (50.4 mg, 0.4 mmol), H_2O (8 mL), K_2CO_3 (27.6 mg, 0.2 mmol). Pd/C@Fe_3O_4 (40 mg), oxygen flow rate (30 mL min^{-1}), 80 ^{o}C, 6 h.

Conclusion

In summary, the Pd/C@Fe_3O_4 catalyst was successfully prepared by the deposition of Pd nanoparticles on the core-shell structure Pd/C@Fe_3O_4 composites and well characterized by TEM, XPS, FT-IR, XRD technologies. The Pd/C@Fe_3O_4 catalyst showed high catalytic activity in the aerobic oxidation of HMF into FDCA in water under mild reaction conditions. It was found the base K_2CO_3 was crucial for the aerobic oxidation of HMF into FDCA. In addition, the base dosage, the reaction temperature and the solvent also showed a great effect on HMF conversion and FDCA yield. Under optimal reaction conditions, HMF conversion of 100% and FDCA yield of 87.8% were obtained after 6 h at 80 ^{o}C. Moreover, the Pd/C@Fe_3O_4 catalyst could be easily separated from the reaction mixture by an external magnet. Compared with other reported methods, our catalytic system shows some distinct advantages: (a) The use of Pd/C@Fe_3O_4 catalyst did not require large amount of base; (b) This method could be conducted under atmospheric oxygen pressure, not requiring the high oxygen pressure; (c) The catalyst could be easily separated by an external magnet and reused without the loss of the catalytic activity. Therefore, the developed method shows a promising potential in the practical production of FDCA from the renewable biomass-based platform chemical.

Acknowledgements

The Project was supported by National Natural Science Foundation of China (No. 21203252 & 21206200), and the Chenguang Youth Science and Technology Project of Wuhan City (No. 2014070404010212).

References

1 P. Gallezot, Chem. Soc. Rev. 2012, **41**, 1538.

2 J. C. Serrano-Ruiz, R. Luque, A. Sepulveda-Escribano, Chem. Soc. Rev. 2011, **40**, 5266.
3 M. E. Zakrzewska, E. Bogel-Łukasik, R. Bogel-Łukasik, Chem. Rev. 2010, **111**, 397.
4 S. Kumar, E. Hablot, J.L.G. Moscoso, W. Obeid, P. G. Hatcher, B. M. DuQuette, D Graiver , R. Narayan , V. Balan, J. Mater. Sci. 2014, **49**, 7824.
5 P. Kangas, I. Hannula, P. Koukkari , M. Hupa, Fuel 2014, **129**, 86.
6 S. P. Simeonov, J. A. S. Coelho, C. A. M. ChemSusChem 2013, **6**, 997.
7 Z. F. Fang, B. Liu, J. J. Luo, Y. S. Ren, Z. H. Zhang, Biomass Bioenerg. 2014, **60**, 171.
8 S. H. Xiao, B. Liu, Y. M. Wang, Z. F. Fang, Z. H. Zhang, Bioresour. Technol. **2014**, **151**, 361.
9 I. Agirrezabal-Telleria, I. Gandarias , P. L. Arias, Catal. Today, 2014, **234**, 42.
10 R. J. van Putten, J. C. van der Waal, E. de Jong, C. B. Rasrendra, H. J. Heeres, J. G. de Vries. Chem. Rev. 2013, **113**, 1499.
11 T. F. Wang, M. W. Nolte, B. H. Shanks, Green Chem. 2014, **16**, 548.
12 Z. H. Zhang, B. Liu, K. L. Lv, J. Sun, K. J. Deng, Green Chem. 2014, **16**, 2762.
13 X. Y. Wan, C. M. Zhou, J. S. Chen, W. P. Deng, Q. H. Zhang, Y. H. Yang, Y. Wang, ACS Catal. 2014, **7**, 2175.
14 Z. H. Zhang, Z. L. Yuan, D. G. Tang, Y. S. Ren, K. L. Lv, B. Liu, ChemSusChem, 2014, DOI: 10.1002/cssc.201402402 .
15 B. S. Wu , Y. T. Xu, Z. Y. Bu, L. B. Wu, B. G. Li , P. Dubois, Polymer 2014, **55**, 3648.
16 A. J. J. E. Eerhart, A. P. C. Faaij, M. K. Patel, Energy Environ. Sci. 2012, **5**, 6407.
17 T. Miura, H. Kakinuma, T. Kawano, H. Matsuhisa, U.S Patent, US-7411078, 2008.
18 W. Partenheimer, V. V. Grushin, Adv. Synth. Catal. 2001, **343**, 102.
19 P .Vinke, W. Van der Poel, H. Van Bekkum, Stud. Surf. Sci. Catal. 1991, **59**, 385.
20 M. Kroger, U. Prusse, K. D.Vorlop, Top. Catal. 2002, **13**, 237.
21 H. A. Rass, N. Essayem, M. Besson, Green Chem. 2013, **15**, 2240.
22 S. E. Davis, L. R. Houk, E. C. Tamargo, A. K. Datye, R. J. Davis, Catal. Today 2011, **160**, 55.
23 O. Casanova, S. Iborra, A. Corma, ChemSusChem 2009, **2**, 1138.
24 S. Davis, B. Zope, R. Davis, Green Chem. 2012, **14**, 143.
25 S. N. Shelke, S. R. Bankar, G. R. Mhaske, S. S. Kadam, D. K. Murade, S. B. Bhorkade, A. K. Rathi, N. Bundaleski, O. M. N. D. Teodoro, R. Zboril, ACS Sustainable Chem. Eng. 2014, **2**, 1699.
26 C. Lei , F. Han , Q. Sun , W. C. Li , A. H. Lu, Chem-A Eur. J. 2014, **20**, 139.
27 M. Y. Zhu, C. J. Wang, D. H. Meng, G. W. Diao, J. Mater. Chem. A, 2013, **1**, 2118.
28 N. Q. Zhao , S. Wu , C. N. He, Z. Y. Wang, C. S. Shi , E. Z. Liu, J. J. Li, Carbon 2013, **57**, 130.
29 I. Do, L.T. Drzal, Carbon 2014, **75**, 43.
30 P. Makowski, R. D. Cakan, M. Antonietti, F. Goettmann, M. M. Titirici, Chem. Commun. 2008, 999.
31 H.G. Wang, L. Sun, Y. P. Li, X. L.Fei , M. D. Sun, C. Q. Zhang, Y. X. Li, Q. B. Yang, Langmuir, 2011, **27**, 11609.
32 K. Jasuja, V. Berry, ACS Nano. 2009, **3**, 2358.
33 Y. H. Kim, M. N. Alam, Y. Marutani, T. Ogata, S. Morisasda, Y. Nakano, Chem. Lett. 2009, **10**, 956.
34 C. Xu, X. Wang, J. Zhu, J. Phys. Chem. C 2008, **112**, 19841.
35 S. H. Xuan, L. Y. Hao, W. Q Jiang, X. L. Gong, Y. Hu, Z. Y. Chen, J. Magn. Magn. Mater. 2007, **308**, 210.
36 X. Sun, Y. D. Li, Angew. Chem. Int. Ed. 2004, **43**, 597.
37 F. Lin, R. Doong, J. Phys. Chem. C 2011, **115**, 6591.
38 Y. M. Lu, H. Z. Zhu, W. G. Li, B. Hu, S. H .Yu, J. Mater. Chem. A 2013, **1**, 3783.
39 G. Kataby, A. Ulman, M. Cojocarua, A. Gedanken , J. Mater. Chem. 1999, **9**, 1501.
40 K. McEleney, C. M. Crudden, J. H. Horton, J. Phys. Chem. C 2009, **113**, 1901.
41 L. Zhang, P. H. Li, J. Yang, M. Wang, L. Wang, ChemPlusChem, 2014, **79**, 217.
42 E. V. Johnston, O. Verho, M. D. Kärkäs, M. Shakeri, C.-W. Tai, P. Palmgren, K. Eriksson, S. Oscarsson, J. E. Bäckvall, Chem-Eur. J. 2012, **18**, 12202.
43 R. R. Sever, T. W. Root , J. Phys. Chem. B 2003, **107**, 4080.
44 H. A. Rass, N. Essayem, M. Besson, Green Chem. 2013, **15**, 2240.
45 K. R. Vuyyuru, P. Strasser, Catal. Today, 2012, **195**, 144.

